Supplementary information

Structure of the polyvinylpyrrolidone-hydrogen peroxide complex

Luke I. Chambers[a], Dmitry S. Yufit[a], Mark A. Fox[a], Osama M. Musa[b], Jonathan W. Steed[a]*

[a] Durham University, Department of Chemistry, Lower Mountjoy, Stockton Road, Durham, DH1 3LE, UK. Email: jon.steed@durham.ac.uk

[b] Ashland LLC, 1005 Route 202/206, Bridgewater, NJ 08807, USA.

Contents

Experimental

Materials and Methods

PVP K-25, PVP K-90, PVP XL-10, PEX K-30, PEX K-90, PEX XL-10 and bisVP were supplied by Ashland LLC. Hydrogen peroxide 30 wt% was purchased from Sigma. All other reagents and solvents were purchased from standard commercial sources and used without further purification. Hydrogen peroxide was handled with care following strict procedures to limit the risk of explosion.[1, 2]

Fourier transform infrared spectra were recorded using a PerkinElmer Spectrum 100 from 4000 – 600 cm^{-1} with an μATR attachment with a resolution of 4 cm^{-1}. Solid-state NMR spectra were recorded at 100.63 MHz using a Bruker Avance III HD spectrometer and a 4 mm magic-angle spinning probe. Spectra were obtained using cross-polarisation with a 3s recycle delay with 1 ms contact time at ambient probe temperature (approx. 25 °C) at a sample spin rate of 10 kHz with 400 repetitions. Spectral referencing was with respect to an external sample of neat tetramethylsilane. Elemental analysis was performed by the University of Durham service using an Exeter CE-440 Elemental Analyser.

Single crystal X-ray crystallography data were collected at 120.0(2) (cocrystals bisVP·H_2O_2·H_2O and bisVP·1.7H_2O_2·0.3H_2O) and 100.0(2)K (cocrystal bisVP·2H_2O_2) on Bruker D8Venture diffractometers (PHOTON III C7 CPAD detector, IμS microsource (bisVP·H_2O_2·H_2O and bisVP·1.7H_2O_2·0.3H_2O); PHOTON III C14 CPAD detector, IμS 3.0 microsource (cocrystal bisVP·2H_2O_2); focusing mirrors, λMoKα, λ = 0.71073 Å) equipped with Cryostream (Oxford Cryostreams) open-flow nitrogen cryostats, and processed using Bruker APEX-III software. The structures were solved using direct methods and refined by full-matrix least squares on

F^2 for all data using SHELXL[3] and OLEX2 software.[4] All non-hydrogen atoms in all structures were refined in anisotropic approximation, hydrogen atoms in structures of bisVP·$2H_2O_2$ and bisVP·H_2O_2·H_2O were located in the difference Fourier maps and refined isotropically. The i.d.p. of hydrogen atoms of water molecule in latter structure were restrained to be identical. Hydrogen atoms in structure bisVP·$1.7H_2O_2$·$0.3H_2O$ were placed into calculated positions and refined in riding mode. OH-distances in this structure were constrained to be the same. The site occupancy factors of disordered atoms in bisVP·$1.7H_2O_2$·$0.3H_2O$ structure were refined but then were rounded to one decimal place and fixed at these values at the final stages of refinement. The final Flack and Hooft parameters in all structures did not allow to establish the absolute structures reliably. X-seed was used to produce an image of the crystal structures for publication.[5] Crystallographic data for the structures have been deposited with the Cambridge Crystallographic Data Centre as supplementary publications CCDC-2088109-2088111.

Titration

Potassium permanganate (3g) was dissolved in distilled water (250 mL) by heating at 100 °C for 1 hour. The solution was filtered, and the volume was made up to 500 mL with distilled water. Oxalic acid (0.05 g) was dissolved in 50 mL distilled water with pure sulfuric acid (0.25 mL) at 60-70 °C. The oxalic acid solution was titrated with the potassium permanganate solution to determine the concentration of the potassium permanganate solution.

The concentration of hydrogen peroxide was increased by storing hydrogen peroxide (20 mL, 30 wt%) in an open beaker in a desiccator (not under vacuum).[6] The desiccant was refreshed weekly. The hydrogen peroxide was left in the desiccator for 55 days with a final concentration of 80 wt%. The concentration was increased further by taking 0.5 ml of the 80 wt % solution and adding ethyl acetate (50 ml x 2) and then removing the solvent under vacuum, to give a final concentration of 85 wt %.

The hydrogen peroxide concentration of both the hydrogen peroxide solution and the PEX samples were determined by dissolving the sample in distilled water (71.25 mL) with sulfuric acid (3.75 mL). The amount of sample used for the hydrogen peroxide solution was 50 µL and for the PEX sample 50 mg. The hydrogen peroxide solution was titrated with the potassium permanganate solution until the solution no longer remained colourless.

BisVP H_2O_2 cocrystal synthesis

The amorphous bisVP hydrogen peroxide complex was prepared by dissolving bisVP (200 mg) and hydrogen peroxide (80 wt%, 60 µL) in ethyl acetate (10 mL). The solvent was removed under vacuum leaving an amorphous paste which was characterised by FTIR spectroscopy.

The crystalline bisVP·1.7H_2O_2·0.3H_2O was prepared by mixing bisVP (50 µL) with hydrogen peroxide (80 wt%, 10 µL) (1:1.36 ratio of bisVP:H_2O_2) and storing at –28 °C. After 2 weeks solid crystalline material formed and was analysed by FTIR spectroscopy. The same quantities of bisVP and hydrogen peroxide were dissolved in different amounts of ethanol (25, 50, 100 µL) and the solid crystalline material was used as a seed crystal. After two hours small colourless block crystals formed. Crystal data: $C_{12}H_{24}N_2O_{5.7}$ M = 287.53 g mol^{-1}, 0.22 × 0.05 × 0.016 mm^3, monoclinic, space group $P2_1$, a = 6.9035(8) Å, b = 15.0032(17) Å, c = 7.0706(8) Å, β = 105.825(4)°, V = 704.58(14) Å^3, Z = 2, D_c = 1.355 g cm^{-3}, F_{000} = 311.0, 11274 reflections collected, 3733 unique (R_{int} = 0.0440). Final GooF = 1.035, R_1 = 0.0456 (3158 reflections with $I \geq 2\sigma(I)$), wR_2 = 0.1028 (all data); 205 parameters, 22 restraints, µ = 0.107 mm^{-1}.

An alternative non-disordered structure refinement was attempted in which the mixed H_2O_2 site was treated as being occupied only by H_2O_2. This refinement resulted in unusually large a.d.p of oxygen atoms of peroxide molecule on the disordered site and an unfeasibly short O–O bond length of 1.315(6) Å and final R_1 = 0.0573. DFT calculations confirmed that such a short bond length is less stable than the equilibrium geometry by 9 kcal mol^{-1} at the MP2/aug-cc-pvdz level. For these reasons the disordered model was adopted. This mixed model is also consistent with the isolation of the non-disordered bisVP·H_2O_2·H_2O.

The crystalline bisVP·H_2O_2·H_2O was prepared by mixing bisVP (100 µL) with hydrogen peroxide (80 wt%, 10 µL) (1:0.68 ratio of bisVP:H_2O_2), a single strand of hair was added to act a seed and the solution was stored at –28 °C. After 1 week solid crystalline material formed and was analysed by FTIR spectroscopy. The same quantities of bisVP and hydrogen peroxide were dissolved in different amounts of ethanol (25, 50, 100 µL) and the solid crystalline material was used as a seed crystal. After two hours small colourless plate crystals formed. Crystal data: $C_{12}H_{24}N_2O_5$ M = 276.33 g mol^{-1}, 0.19 × 0.13 × 0.09 mm^3, monoclinic, space group $P2_1$, a = 6.9359(3) Å, b = 14.9061(7) Å, c = 6.9555(3) Å, β =

105.7571(17)°, V = 692.12(5) Å^3, Z = 2, D_c = 1.326 g cm^{-3}, F_{000} = 300.0, 11754 reflections collected, 4014 unique (R_{int} = 0.0346). Final GooF = 1.026, R_1 = 0.0448, *(*3711 reflections with $I \geq 2\sigma(I)$) wR_2 = 0.1136 (all data);267 parameters, 1 restraint, μ = 0.102 mm^{-1}.

The crystalline bisVP·2H_2O_2 was prepared by mixing bisVP (25 μL) with hydrogen peroxide (85wt%, 10.2 μL) (1:3.17 ratio of bisVP:H_2O_2) and storing at –28 °C. The solution was seeded using small crystals of bisVP·1.7H_2O_2:0.3H_2O, causing the solution to crystallise. The solid crystalline material formed was analysed by FTIR spectroscopy. The same quantities of bisVP and hydrogen peroxide were dissolved in different amounts of ethanol (25, 50 μL) and the solid crystalline material was used as a seed crystal. After two hours small colourless plate crystals formed. Crystal data: $C_{12}H_{24}N_2O_6$ M = 292.33 g mol^{-1}, 0.21 × 0.09 × 0.04 mm^3, monoclinic, space group $P2_1$, a = 6.8700(2) Å, b = 15.0114(4) Å, c = 7.1364(2) Å, β = 105.8830(10)°, V = 707.87(3) Å^3, Z = 2, D_c = 1.372 g cm^{-3}, F_{000} = 316.0, 16854 reflections collected, 4085 unique (R_{int} = 0.0322). Final GooF = 1.056, R_1 = 0.0352, *(*3901 reflections with $I \geq 2\sigma(I)$), wR_2 = 0.0858 (all data); 277 parameters, 1 restraint, μ = 0.109 mm^{-1}.

Computations

Geometry optimisations were carried out with the Gaussian 16 package.[7] Ground state (S_0) geometries were fully optimised from starting geometries generated from the initial X-ray structure of BisVP.2H_2O_2 without symmetry constraints at the hybrid-DFT functional B3LYP[8, 9] with the 6-31(d) basis set[10, 11] and the Grimme dispersion factor, GD3BJ.[12] All fully optimised geometries were confirmed as true minima based on no imaginary frequencies found from frequency calculations. Simulated IR spectra were generated from frequency calculations using a scaling factor[13] of 0.95 to compare with experimental IR data. Carbon-13 NMR chemical shifts in ppm (δ) were converted[14] from sigma (σ) values within the calculated GIAO-NMR data for the optimised geometries at B3LYP/6-31G(d)/GD3BJ using the equation δ(^{13}C) = 196-(σ(^{13}C)/0.95) with tetramethylsilane (TMS) as external reference at 0.0 ppm. ^{13}C NMR chemical shifts for CO groups were averaged from the inner non-equivalent CO groups of the geometries.

Limitations of multimolecular models.

PVP/bisVP solids contain many (hundreds) molecules where most molecules are in a very similar environment. Few molecules occupy the edges/surfaces of the solid particle/lattice. In the multimolecular models a proportionally high number of molecules are at the edges of

the ‘sheet’. This means the simulated IR spectra and NMR shifts can vary between those molecules in the ‘centre’ i.e. in the appropriate environment in solids and those on the edges. The simulated IR spectra of bisVP/PVP:H_2O_2/H_2O complexes contain unusual O-H bands which can be due to dangling/edge H_2O_2/H_2O molecules rather than be considered as representative of the solids.

Both hydrogens in a H_2O_2 (and water) molecule are expected to be involved in intermolecular hydrogen bond interactions in the solids of bisVP/PVP:H_2O_2/H_2O complexes. However, in these multimolecular models, several dangling H_2O_2 (H_2O) edge molecules exist where only one hydrogen bond interaction is present per molecule initially and some of these molecules will rearrange to form a second H-bond interaction. The AB motifs have more dangling/edge H_2O_2/H_2O molecules thus less intermolecular hydrogen bond interactions overall and the overall total energy of the model would be higher than the A motifs where there are less dangling/edge molecules initially. So even though the A motifs are more stable energetically than AB motifs based on these models, the energy differences may be attributed to the different edge molecules within.

Supplementary Figures

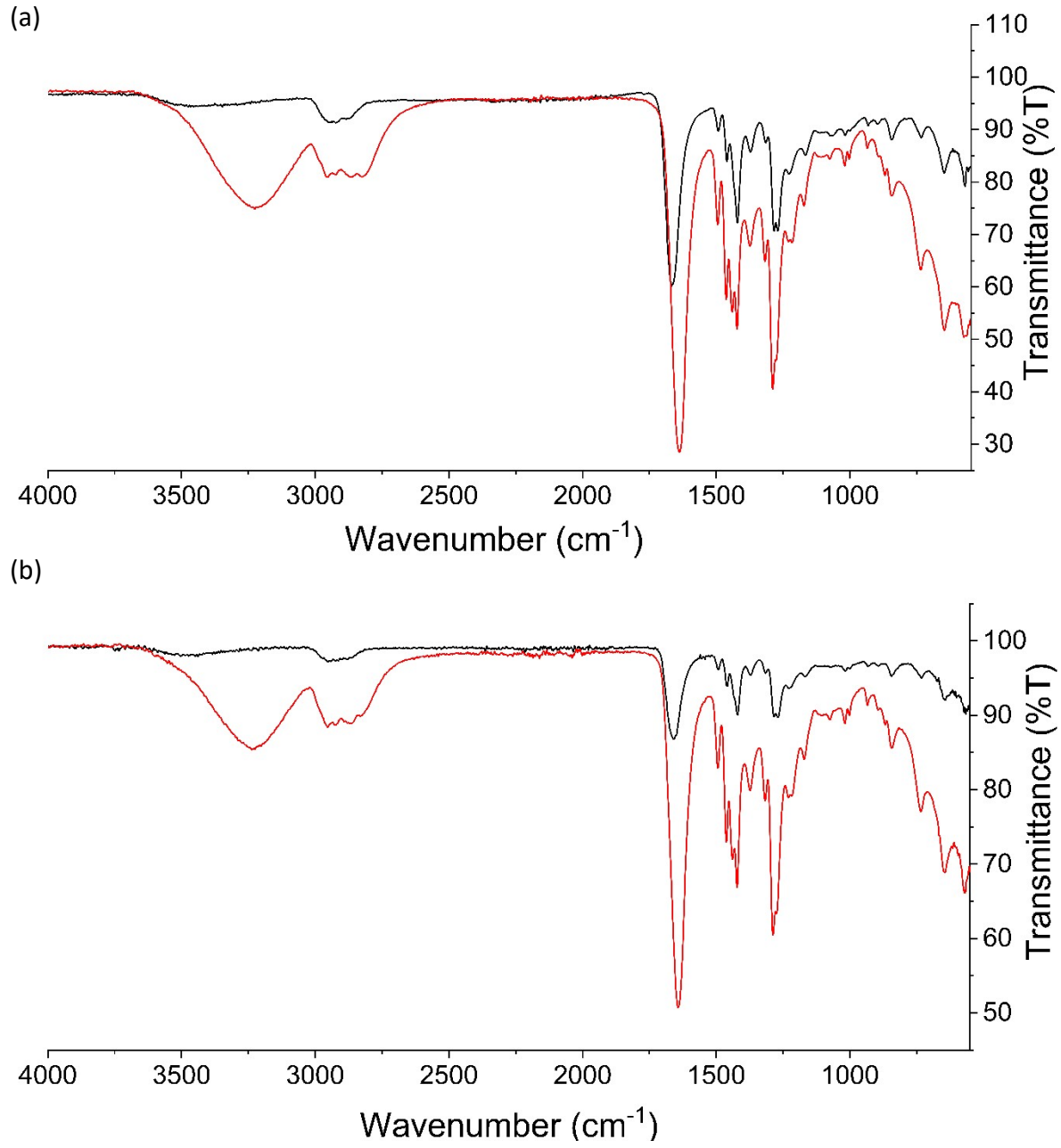

Figure S1. (a) FTIR spectra of PVP K-25 (black) and PEX K-30 (red). (b) FTIR spectra of PVP K-90 (black) and PEX K-90 (red).

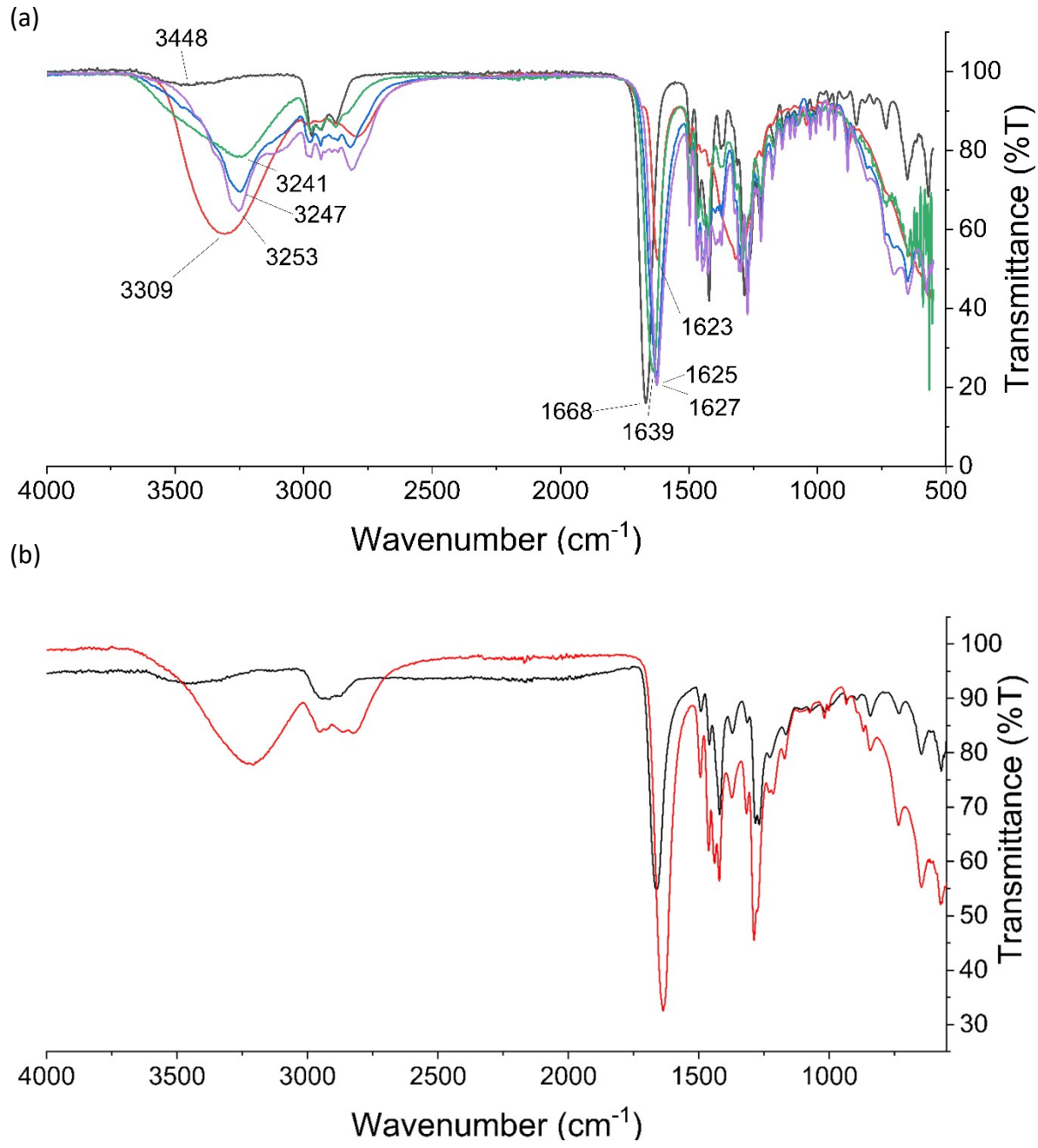

Figure S2. (a) FTIR spectrum of bisVP (black), amorphous bisVP hydrogen peroxide complex (red), bisVP·H_2O_2·H_2O (green), bisVP·1.7H_2O_2·0.3H_2O (purple) and bisVP·2H_2O_2 complex (blue). (b) The FTIR spectra of PVP XL-10 (black) and PEX XL-10 (red).

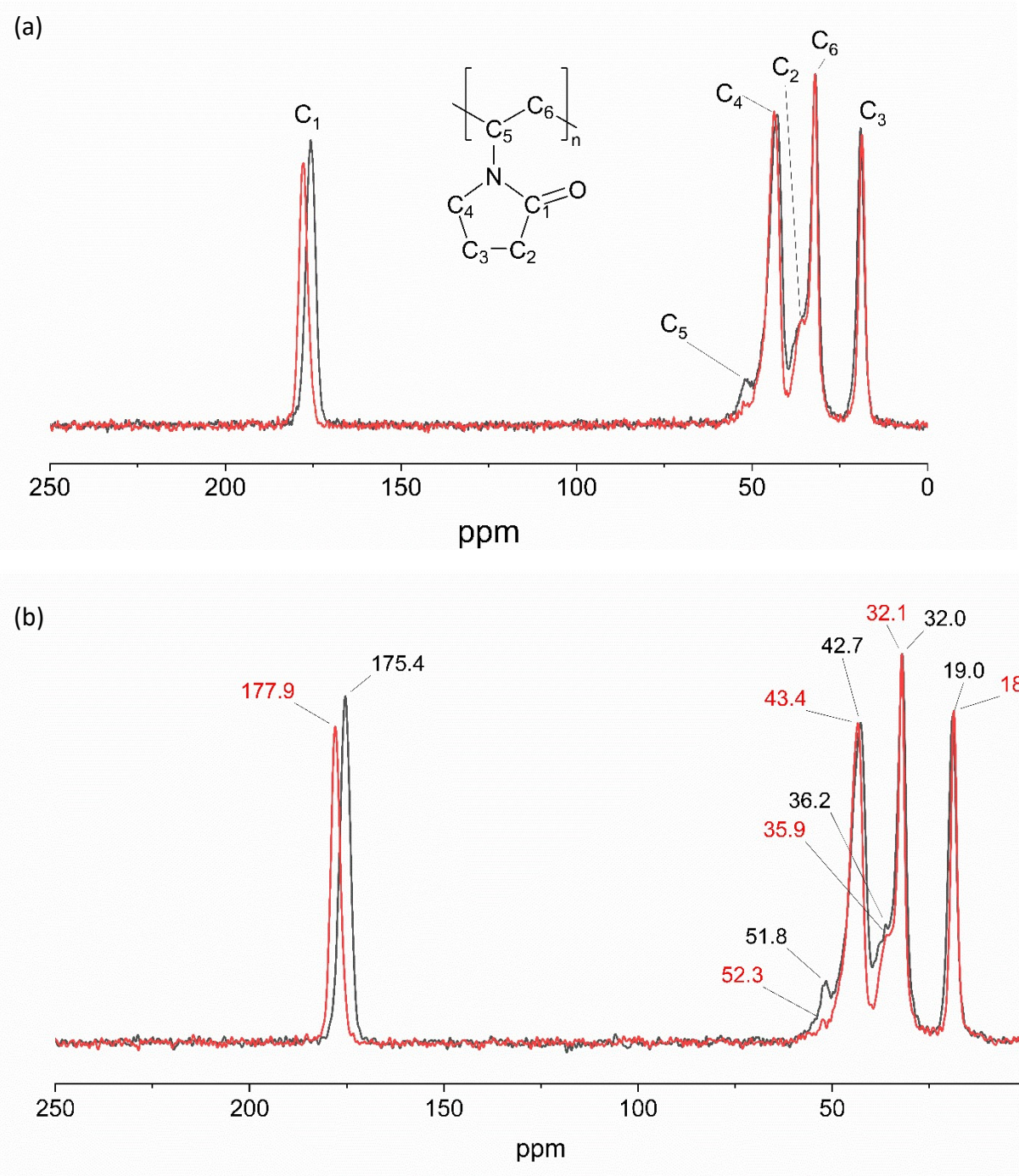

Figure S3. (a) The MAS solid state NMR spectra of PVP K-25 (black) and PEX K-30 (red) (b) The MAS solid state NMR of PVP K-90 (black) and PEX K-90 (red).

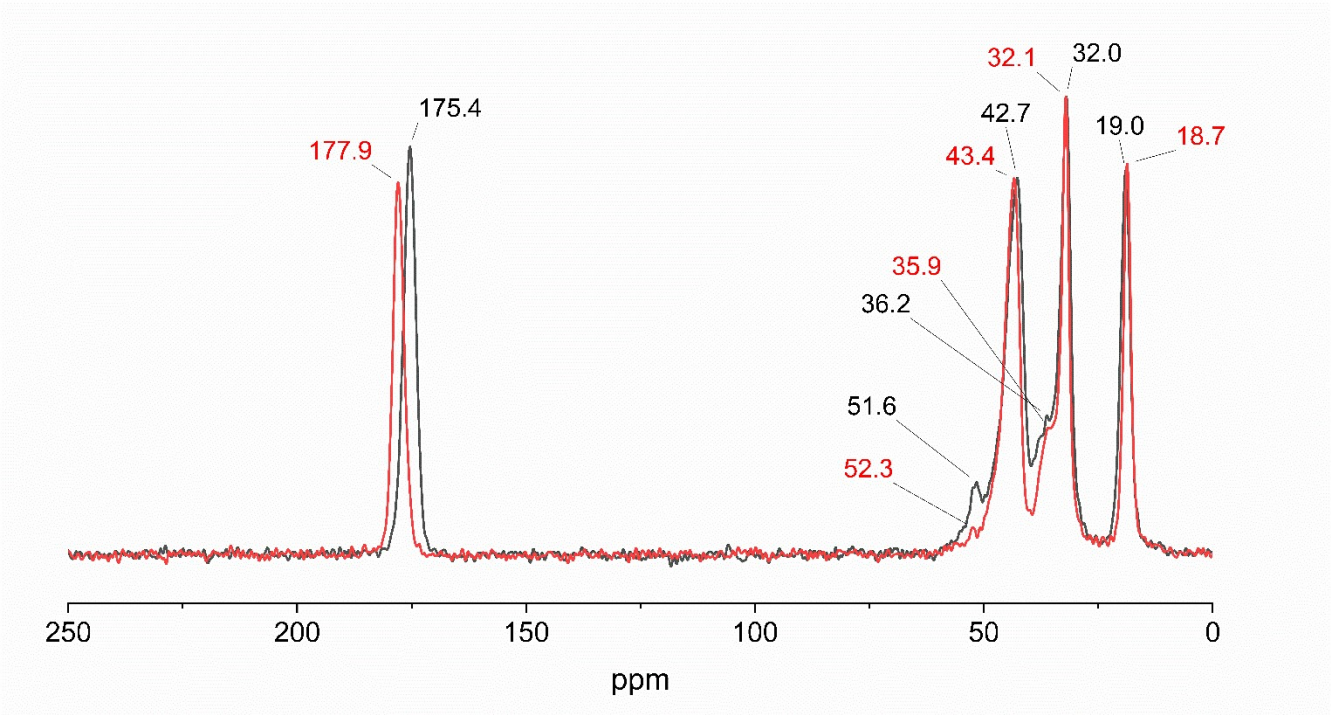

Figure S4. The MAS solid state NMR of PVP XL-10 (black) and XL-10 (red).

Sample	Stretching band (cm^{-1})	
	vOH	vCO
PVP K-25	3458	1667
PEX K-30	3226	1638
PVP K-90	3460	1659
PEX K-90	3238	1642
PVP XL-10	3460	1663
PEX XL-10	3206	1637
BisVP	3448	1668
BisVP-H_2O_2 amorphous	3309	1623
BisVP·H_2O_2·H_2O	3241	1639
BisVP·1.7H_2O_2·0.3H_2O	3247	1627
BisVP·2H_2O_2	3253	1625

Table S1. FTIR vOH and vCO stretching bands for PVP K-25, K-90 XL-10, PEX K-30, K-90, XL-10, bisVP, amorphous bisVP-H_2O_2 and crystalline bisVP·2H_2O_2.

Sample	Mass of sample/ g	Volume/mL	Conc. of potassium permanganate	wt% H_2O_2	Ratio of H_2O_2 (x) to VP (1)
PEX K-30	0.0515	4.4	2.58E-05	18.73	0.75
PEX K-30	0.0510	5.2	2.58E-05	22.35	0.94
PEX K-30	0.0497	4.8	2.58E-05	21.17	0.88
			average	20.75	0.86
PEX K-90	0.0509	4	2.58E-05	17.22	0.68
PEX K-90	0.0512	4	2.58E-05	17.12	0.68
PEX K-90	0.0505	4	2.58E-05	17.36	0.69
			average	17.24	0.68
PEX XL-10	0.0514	4.6	2.58E-05	19.61	0.80
PEX XL-10	0.0504	4.2	2.58E-05	18.26	0.73
PEX XL-10	0.0511	4.4	2.58E-05	18.87	0.76
			average	18.92	0.76

Table S2. Table of all titration results including calculated weight percentage of hydrogen peroxide and calculated ratio of hydrogen peroxide to VP (assuming no water present in peroxydone).

Sample	Sample no.	Elemental percentage			Calculated H_2O content			
		%C	%H	%N	%C	%H	%N	Average
PVP K-25	1	60.10	8.24	11.24	0.49	0.16	0.75	
	2	60.46	7.79	11.83	0.45	0.68	0.40	
	3	60.01	7.68	11.73	0.50	0.85	0.46	
	Av	60.19	7.90	11.60	0.48	-0.45	0.54	0.19
PVP K-90	1	61.51	8.18	11.56	0.33	0.04	0.56	
	2	61.65	7.83	11.96	0.32	0.61	0.33	
	3	60.78	7.75	11.79	0.41	0.74	0.43	
	Av	61.31	7.92	11.77	0.36	-0.44	0.44	0.12
PVP XL-10	1	60.91	8.21	11.43	0.40	0.10	0.63	
	2	60.20	7.65	11.63	0.48	0.89	0.52	
	3	59.68	7.55	11.54	0.53	1.04	0.57	
	Av	60.26	7.80	11.53	0.47	-0.61	0.57	0.14

Table S3. Table of the elemental analysis results for PVP K-25, K-90 and XL-10 including average result and calculated water content based on the elemental percentages for carbon, hydrogen, and nitrogen.

Sample	Expected		
	%C	%H	%N
PVP	64.84	8.16	12.6
PVP + 0.5 H_2O	59.98	8.39	11.66
PVP + 0.25 H_2O	62.31	8.28	12.11

Table S4. Table of the expected elemental analysis values with of PVP with two different ratios of PVP monomer to water molecule.

Sample	Sample no.	Elemental percentage			Calculated H_2O_2 content
		%C	%H	%N	
PEX K30	1	51.76	7.81	9.63	0.83
	2	50.73	7.43	9.88	0.91
	3	50.30	7.30	9.80	0.94
	Av	50.93	7.51	9.77	0.89
PEX K90	1	52.39	7.92	9.87	0.78
	2	52.41	7.43	10.19	0.77
	3	52.44	7.41	10.19	0.77
	Av	52.41	7.59	10.08	0.77
PEX XL10	1	50.54	7.77	9.45	0.92
	2	50.69	7.34	9.80	0.91
	3	50.69	7.33	9.79	0.91
	Av	50.64	7.48	9.68	0.92

Table S5. Table of the elemental analysis results for PEX K-30, K-90 and XL-10 including average result and calculated hydrogen peroxide content per monomer unit based on the elemental percentages for carbon (assuming no water is present).

Sample	Ratio (H_2O_2 to C=O)	Expected		
		%C	%H	%N
PEX (1 H_2O_2)	(1:1)	49.64	7.64	9.65
PEX (0.5 H_2O_2)	(1:2)	56.23	7.87	10.93
PEX (0.75 H_2O_2)	(3:4)	52.73	7.75	10.25

Table S6. Table of the expected elemental analysis values with of PEX with three different ratios of PVP monomer to hydrogen peroxide molecule.

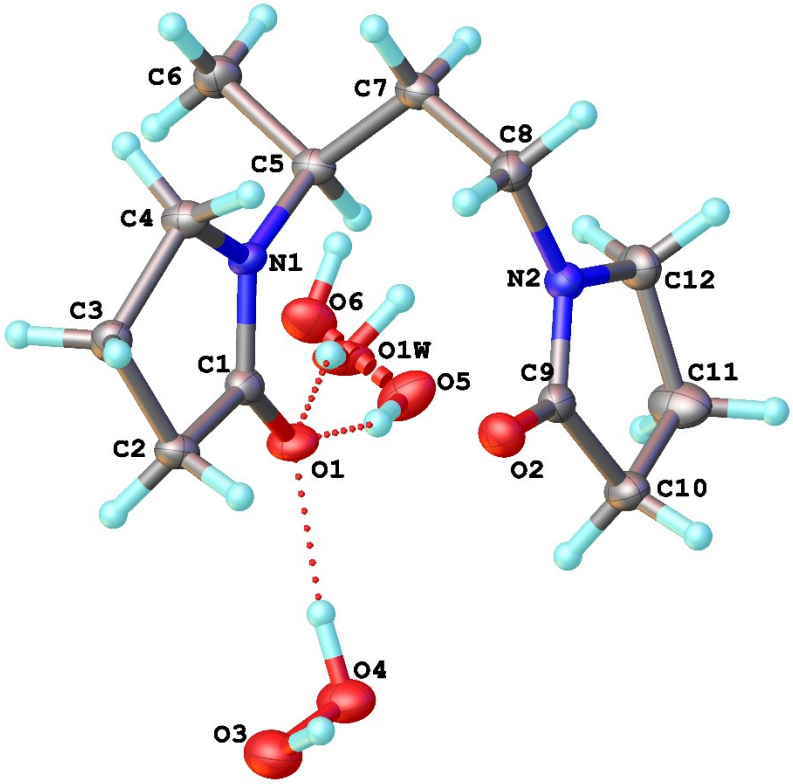

Figure S5. Crystal structure of BisVP·1.7H_2O_2·0.3H_2O showing the disorder in one of the hydrogen peroxide molecules.

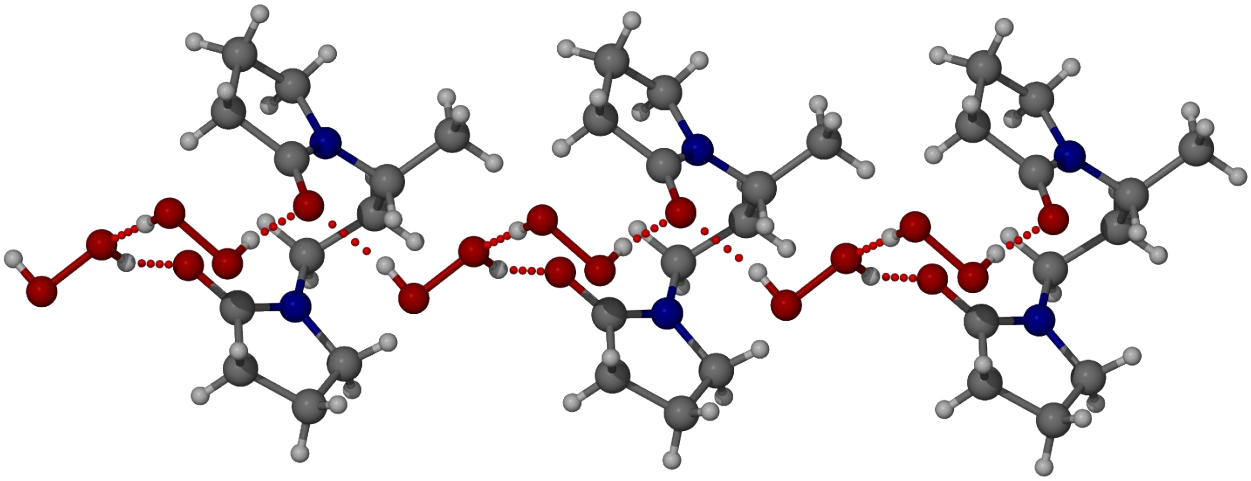

Figure S6. Extended crystal structure of BisVP·2H_2O_2.

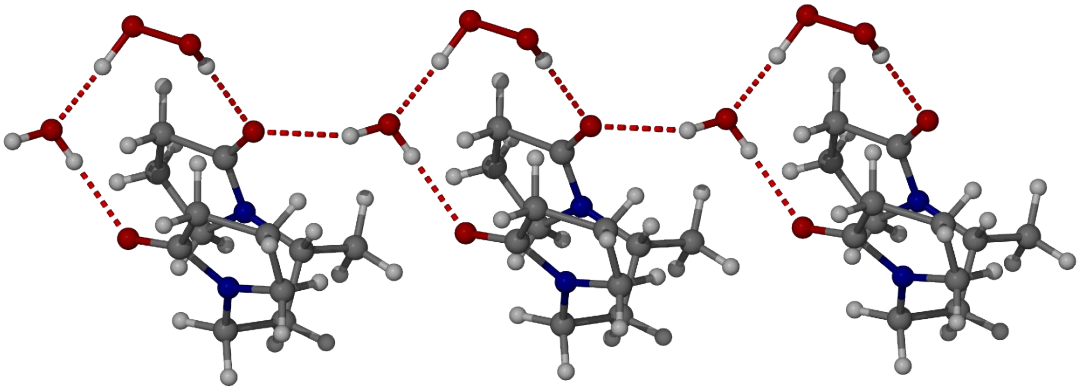

Figure S7. Extended crystal structure of BisVP·H_2O_2·H_2O.

	Electronic Energy a.u.	Gibbs Free Energy a.u.	ν(OH) cm^{-1}	ν(CO) cm^{-1}	δ(^{13}C) CO ppm
BisVP Geometries					
6 BisVP molecules	-4376.494854	-4374.723144		1682	172.6
6 BisVP molecules, 12 H_2O molecules, 2 AB-ribbons	-5293.759649	-5291.703330	3441	1643	176.9
6 BisVP molecules, 6 H_2O molecules at B, 6 H_2O_2 molecules at A, 2 AB-ribbons	-5744.551433	-5742.479169	3405	1633	177.9
6 BisVP molecules, 6 H_2O molecules at A, 6 H_2O_2 molecules at B, 2 AB-ribbons	-5744.529388	-5742.463241	3253	1641	176.8
6 BisVP molecules, 12 H_2O_2 molecules, 2 AB-ribbons	-6195.318765	-6193.232706	3311	1637	178.4
6 BisVP molecules, 12 H_2O_2 molecules, 2 A-ribbons	-6195.328817	-6193.239362	3191	1652	177.2
6 BisVP molecules, 12 H_2O_2 molecules, 3 A-ribbons	-6195.328154	-6193.240773	3243	1644	176.3
2 BisVP molecules, 4 H_2O_2 molecules, 1 A-ribbon	-2065.072806	-2064.395689	3316	1655	177.1
3 BisVP molecules, 6 H_2O_2 molecules, 1 A-ribbon	-3097.632697	-3096.603071	3234	1655	178.1
PVP Tetramer Geometries					
3 PVP4 molecules	-4372.869170	-4371.149970		1690	173.7
3 PVP4 molecules, 12 H_2O molecules, 2 AB-ribbons	-5290.113263	-5288.109508	3471	1655	176.5
3 PVP4 molecules, 6 H_2O molecules at B, 6 H_2O_2 molecules at A, 2 AB-ribbons	-5740.953063	-5738.918928	3220	1650	175.4
3 PVP4 molecules, 6 H_2O molecules at A, 6 H_2O_2 molecules at B, 2 AB-ribbons	-5740.936069	-5738.915407	3132	1645	176.6
3 PVP4 molecules, 12 H_2O_2 molecules, 2 AB-ribbons	-6191.678206	-6189.644835	3293	1643	177.8
3 PVP4 molecules, 12 H_2O_2 molecules, 2 A-ribbons	-6191.702085	-6189.667176	3149	1649	178.1
3 PVP4 molecules, 12 H_2O_2 molecules, 3 A-ribbons	-6191.710058	-6189.670600	3190	1647	177.7
PVP Hexamer Geometries					
2 PVP6 molecules	-4371.498830	-4369.784722		1688	174.4
2 PVP6 molecules, 12 H_2O_2 molecules, 2A-ribbons	-6190.481146	-6188.460352	3300	1652	179.0
1 PVP6 molecule	-2185.818454	-2184.977586		1698	174.1
1 PVP6 molecule, 6 H_2O_2 molecules, 1A-ribbon	-3095.227374	-3094.229528	3290	1654	178.9

Table S7. Table of calculated total energies, predicted OH and CO stretching IR bands and ^{13}C NMR chemical shifts of CO for the optimised geometries in this study.

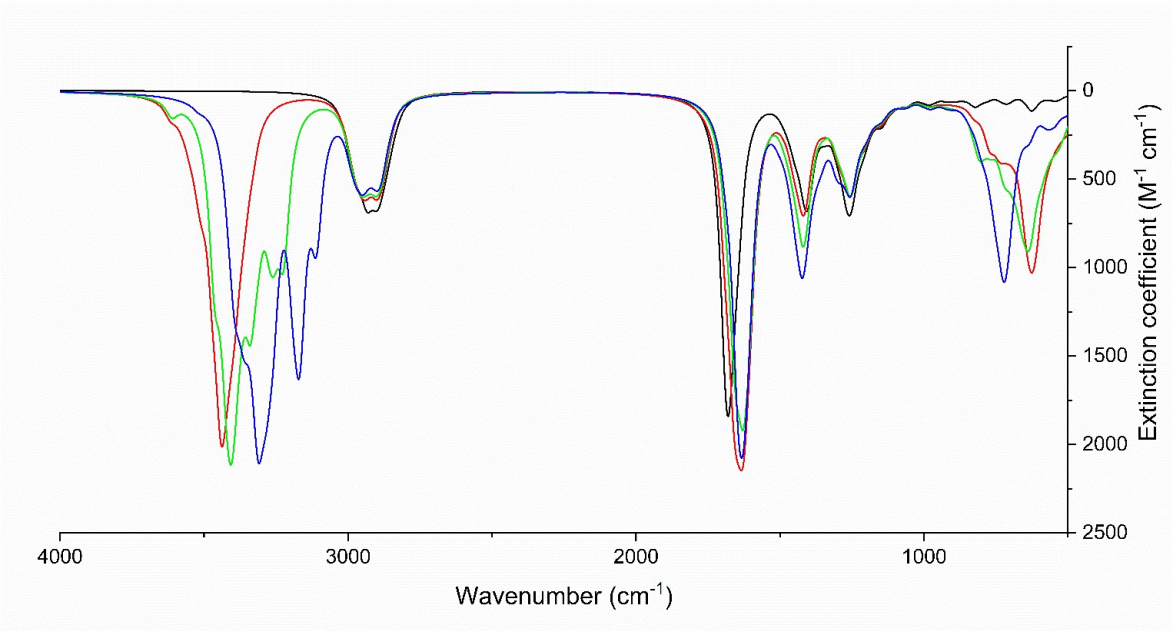

Figure S8. Simulated IR spectra for models with 6 bisVP molecules. Pure bisVP is shown in black, bisVP·2H_2O in red, bisVP·H_2O·H_2O_2 in green and bisVP·2H_2O_2 in blue. The H_2O_2 and water complexes contain the AB hydrogen bonding motifs.

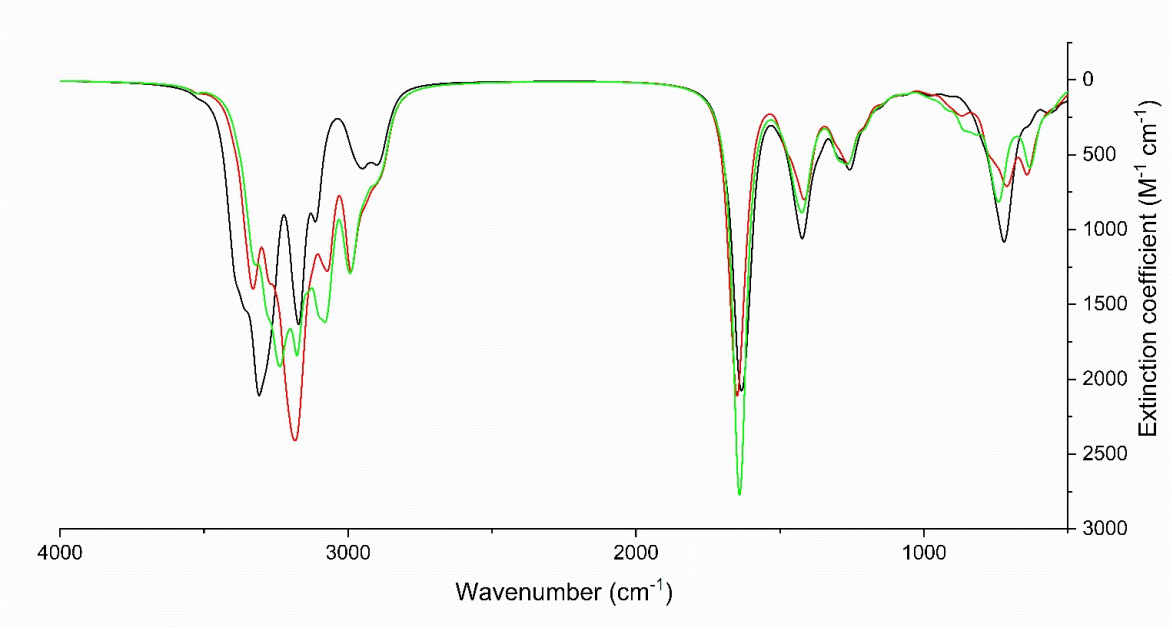

Figure S9. Simulated IR spectra for models with 6 bisVP molecules and 12 H_2O_2 molecules with different hydrogen bonding motifs. The AB motif is shown in black, the A motif with two ribbons is shown red and the A motif with three ribbons is shown in green.

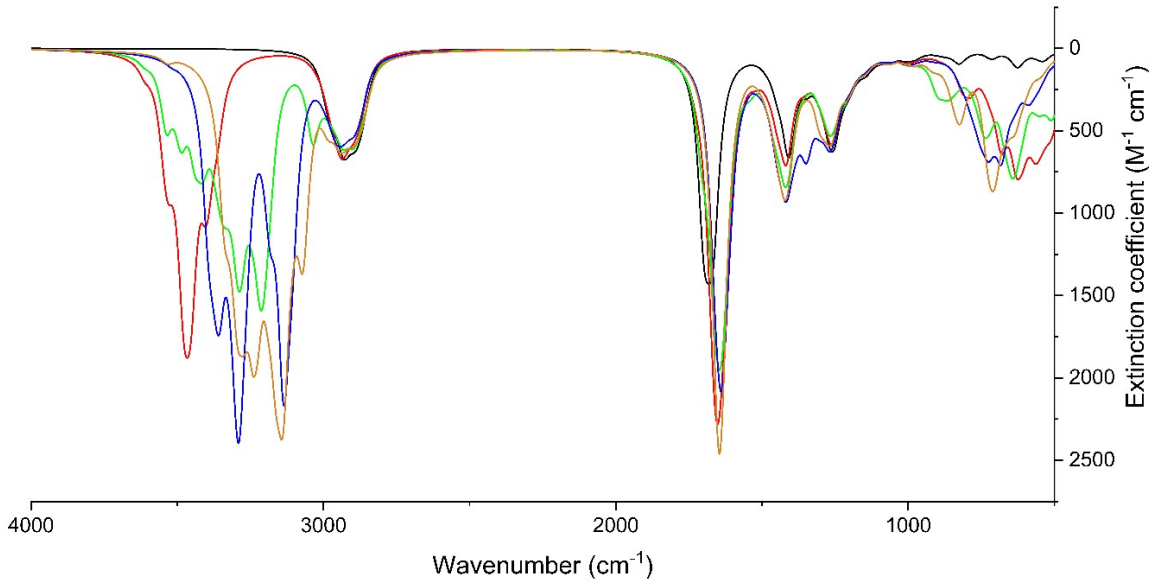

Figure S10. Simulated IR spectra for models with PVP tetramer (PVP4) molecules. Pure PVP4 is shown in black, 3PVP4·12H_2O with two AB ribbons is shown in red, 3PVP4·6H_2O·6H_2O_2 with two AB ribbons is shown in green, 3PVP4·12H_2O_2 with two AB ribbons in blue and 3PVP4·12H_2O_2 with 2 A ribbons in orange.

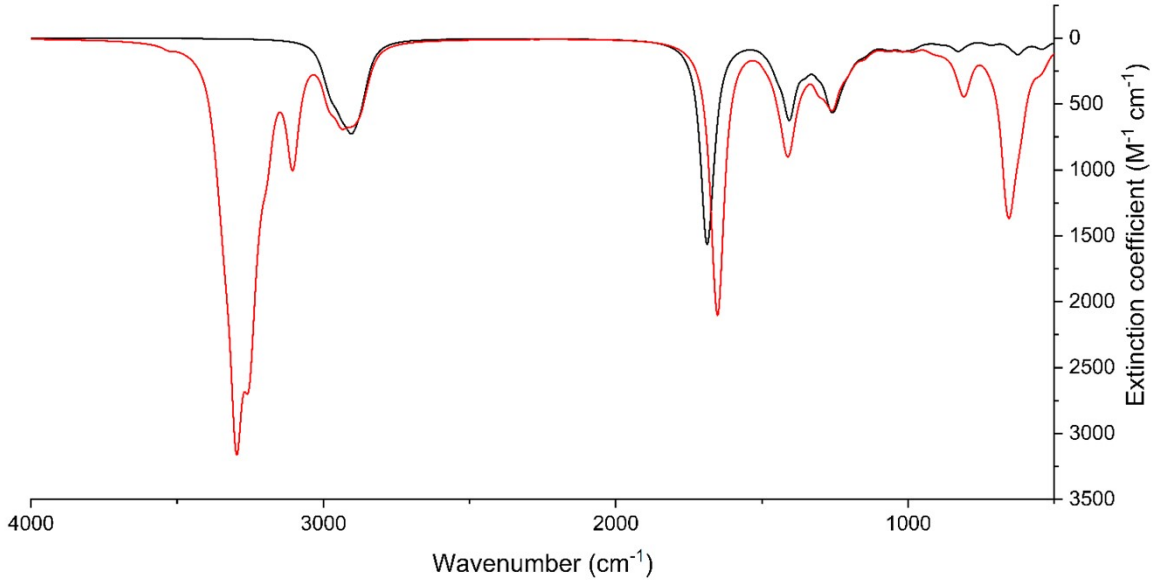

Figure S11. Simulated IR spectra for models with PVP hexamer (PVP6) molecules. Pure PVP6 is shown in black and 2PVP6·12H_2O_2 with two A ribbons is shown in red.

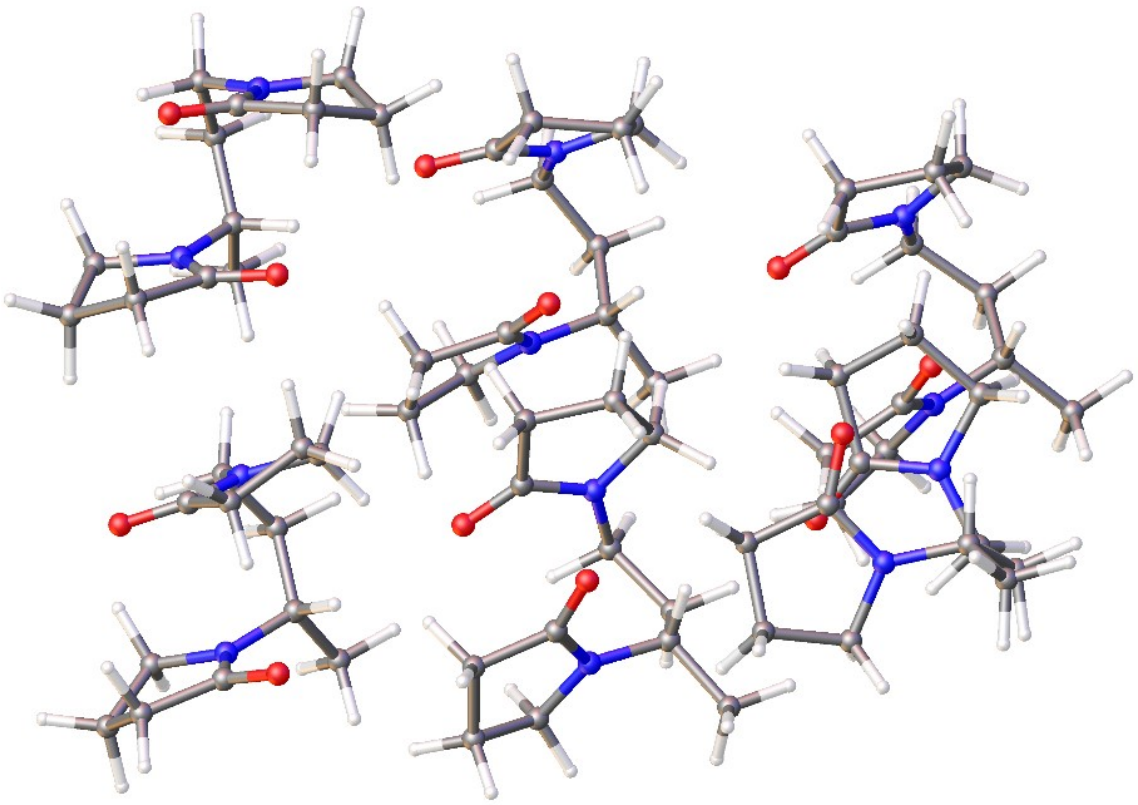

Figure S12. The DFT calculated structure of six bisVP molecules.

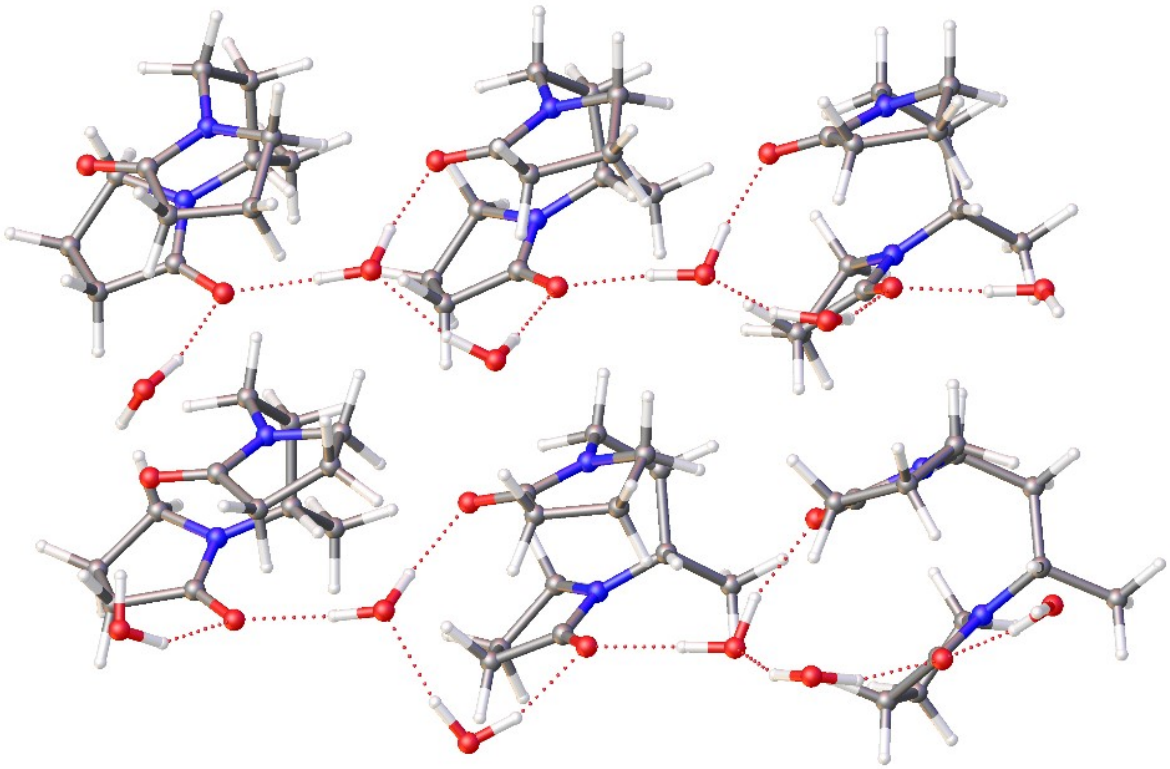

Figure S13. The DFT calculated structure of six bisVP molecules with twelve water molecules forming two AB-ribbons.

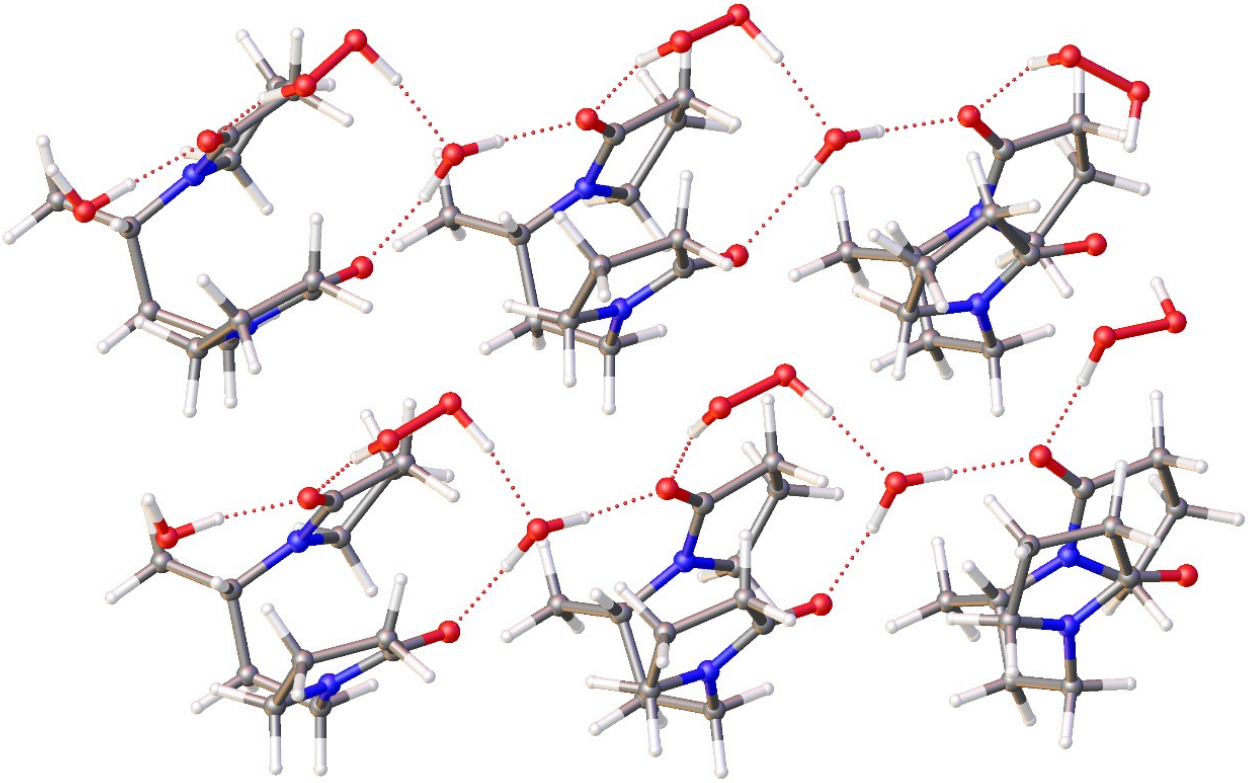

Figure S14. The DFT calculated structure of six bisVP molecules with six water molecules at position B and six H_2O_2 molecules at position A, forming two AB-ribbons.

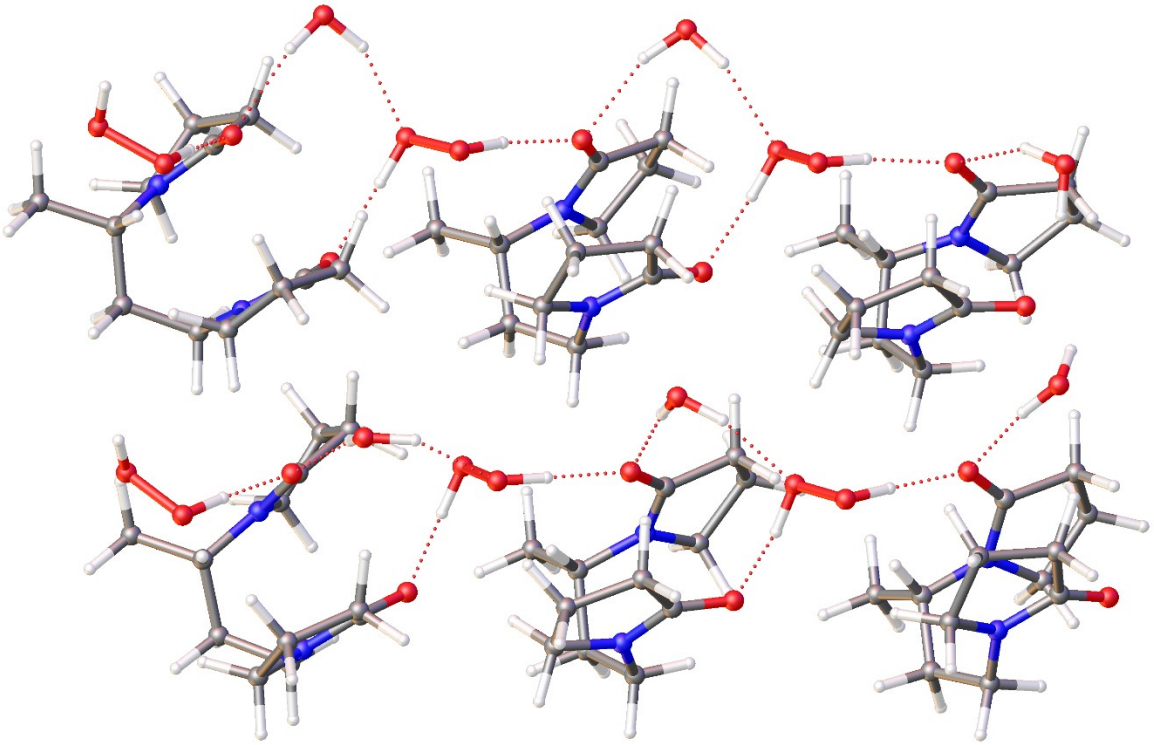

Figure S15. The DFT calculated structure of six bisVP molecules with six water molecules at position A and six H_2O_2 molecules at position B, forming two AB-ribbons.

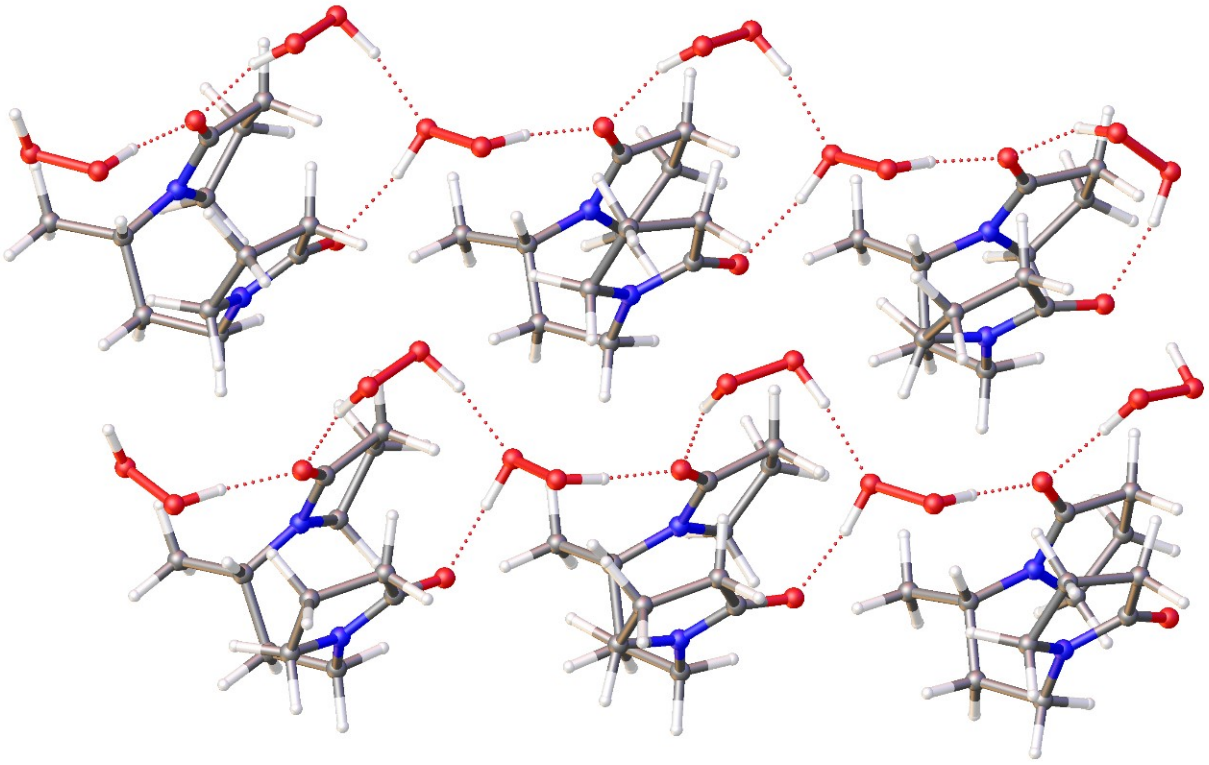

Figure S16. The DFT calculated structure of six bisVP molecules with twelve H_2O_2 molecules, forming two AB-ribbons.

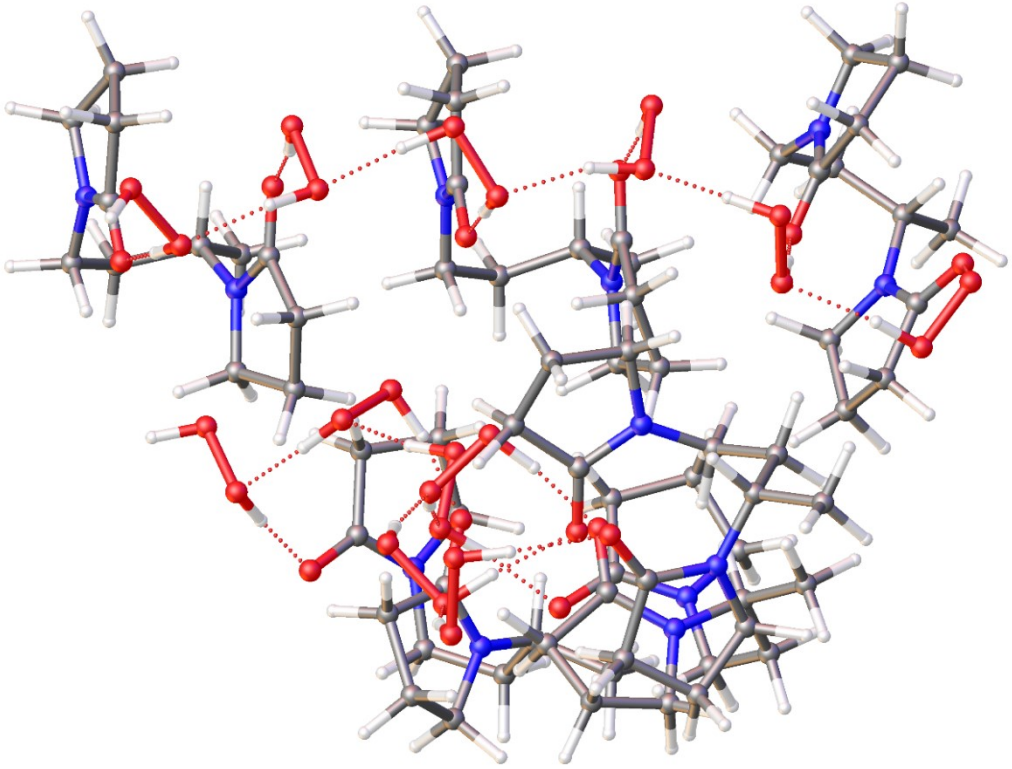

Figure S17. The DFT calculated structure of six bisVP molecules with twelve H_2O_2 molecules, forming two all-A ribbons.

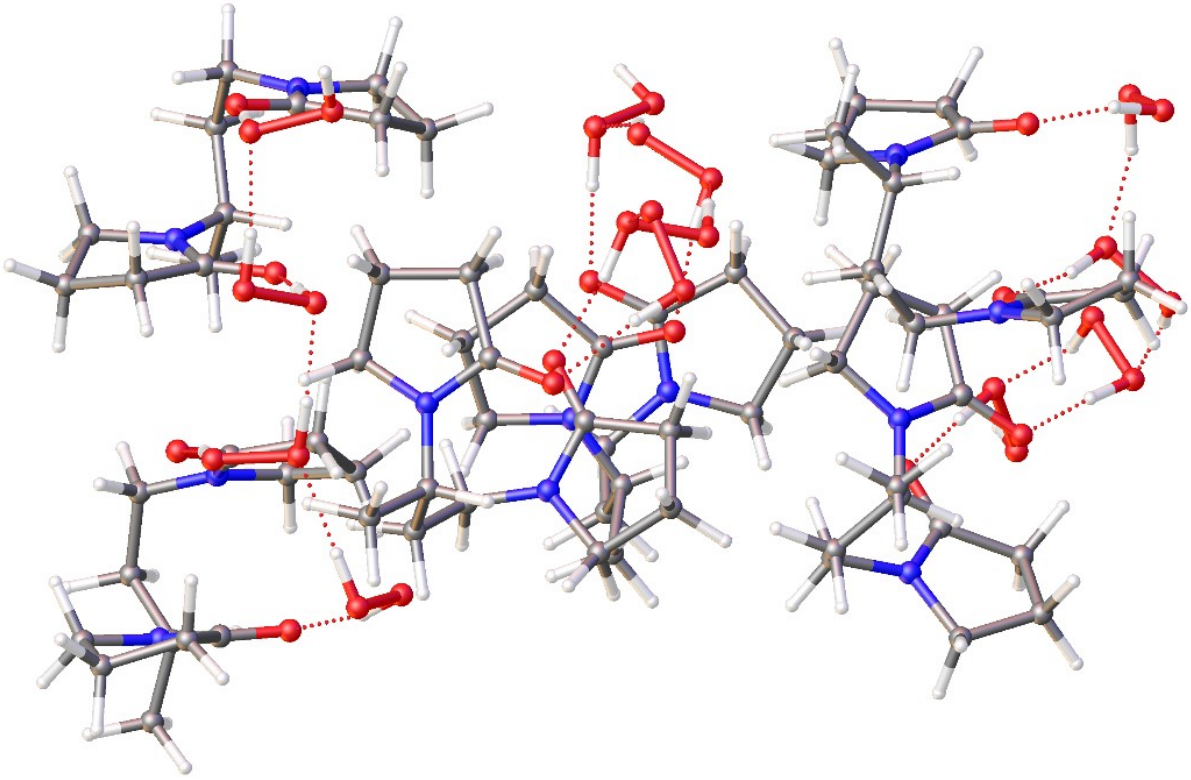

Figure S18. The DFT calculated structure of six bisVP molecules with twelve H_2O_2 molecules, forming three all-A ribbons.

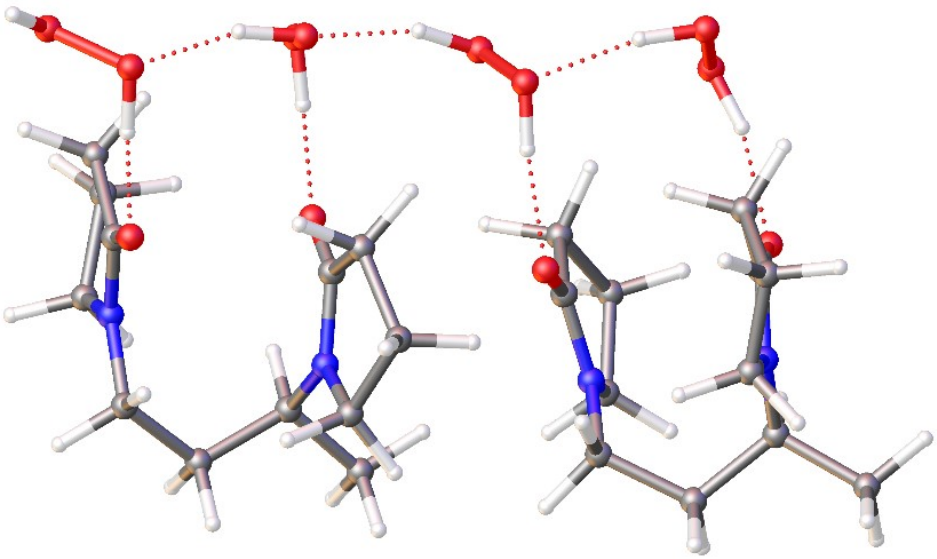

Figure S19. The DFT calculated structure of two bisVP molecules with four H_2O_2 molecules, forming one all-A ribbons.

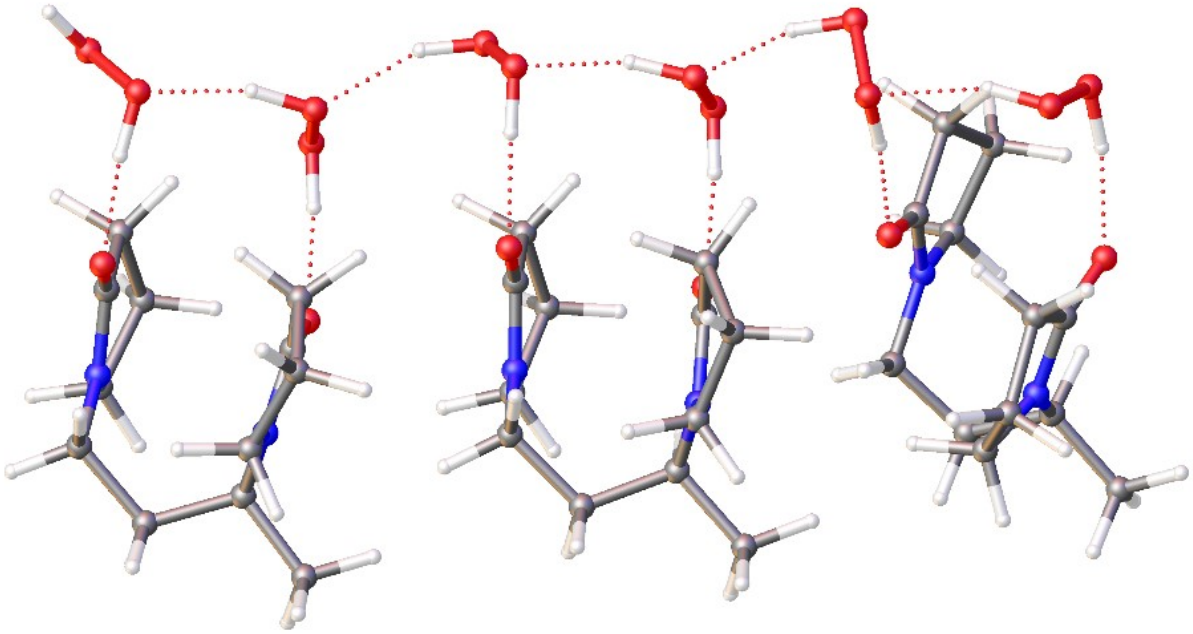

Figure S20. The DFT calculated structure of three bisVP molecules with six H_2O_2 molecules, forming one all-A ribbons.

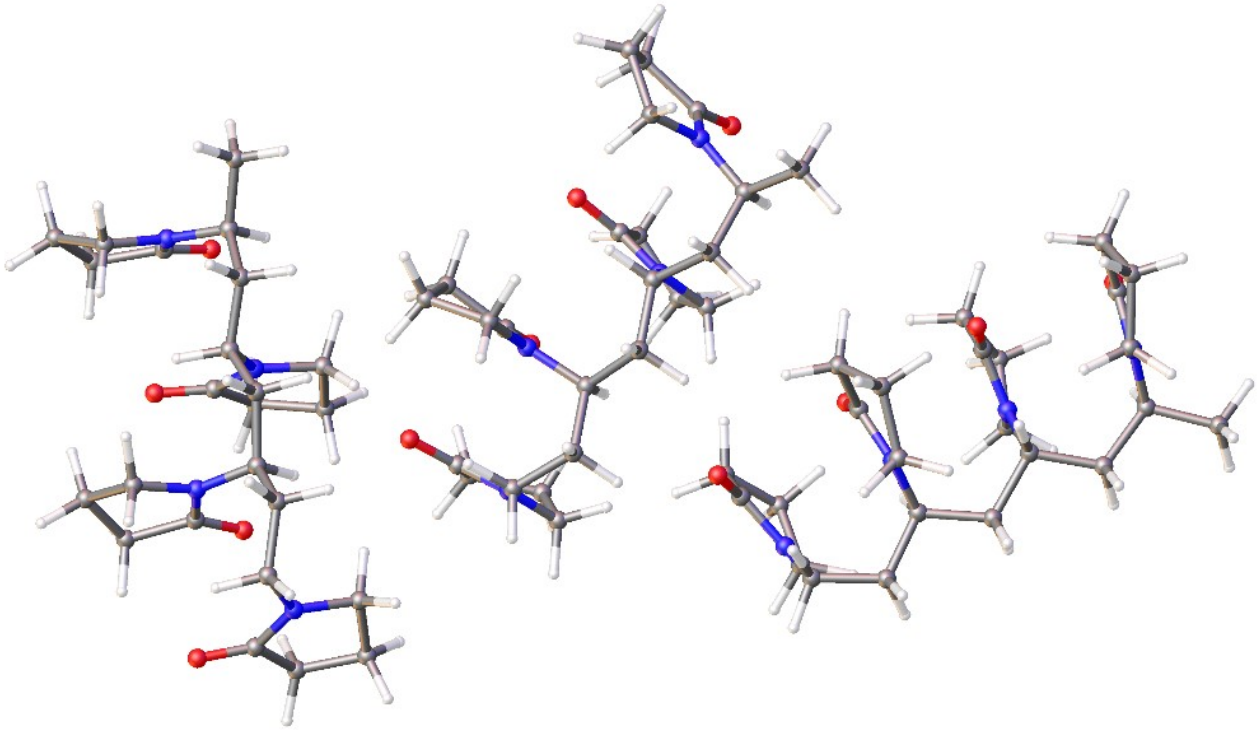

Figure S21. The DFT calculated structure of three PVP tetramer molecules.

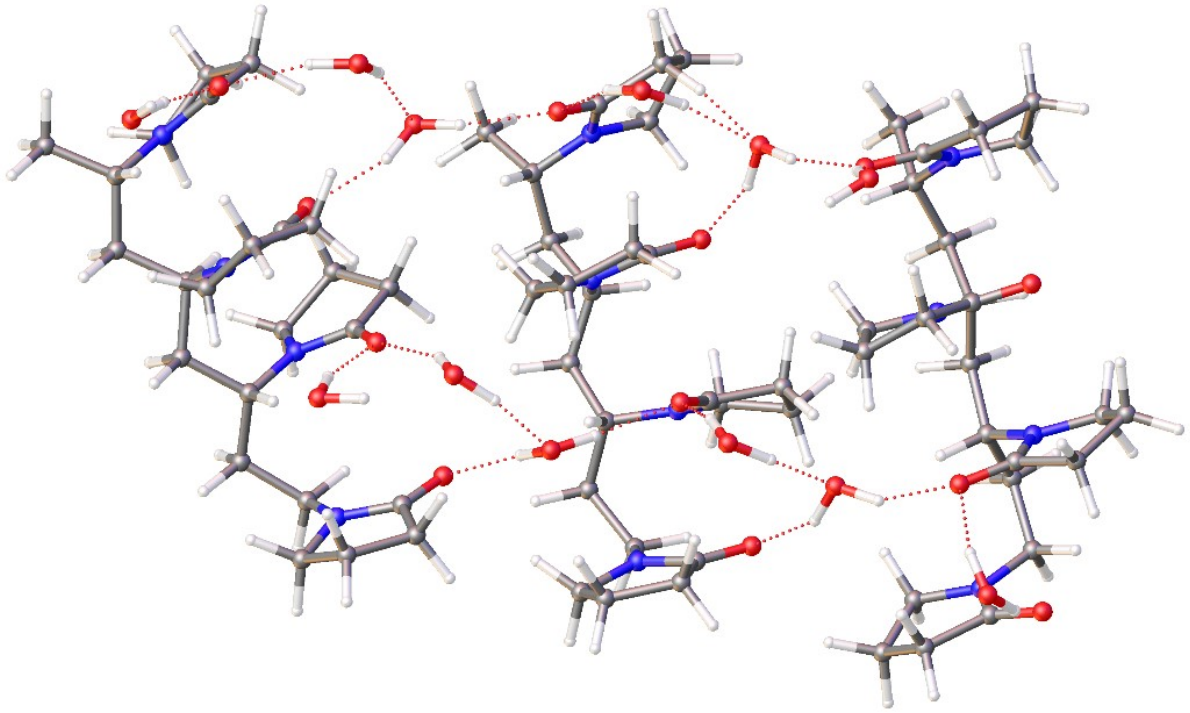

Figure S22. The DFT calculated structure of three PVP tetramer molecules with twelve water molecules, forming two AB ribbons.

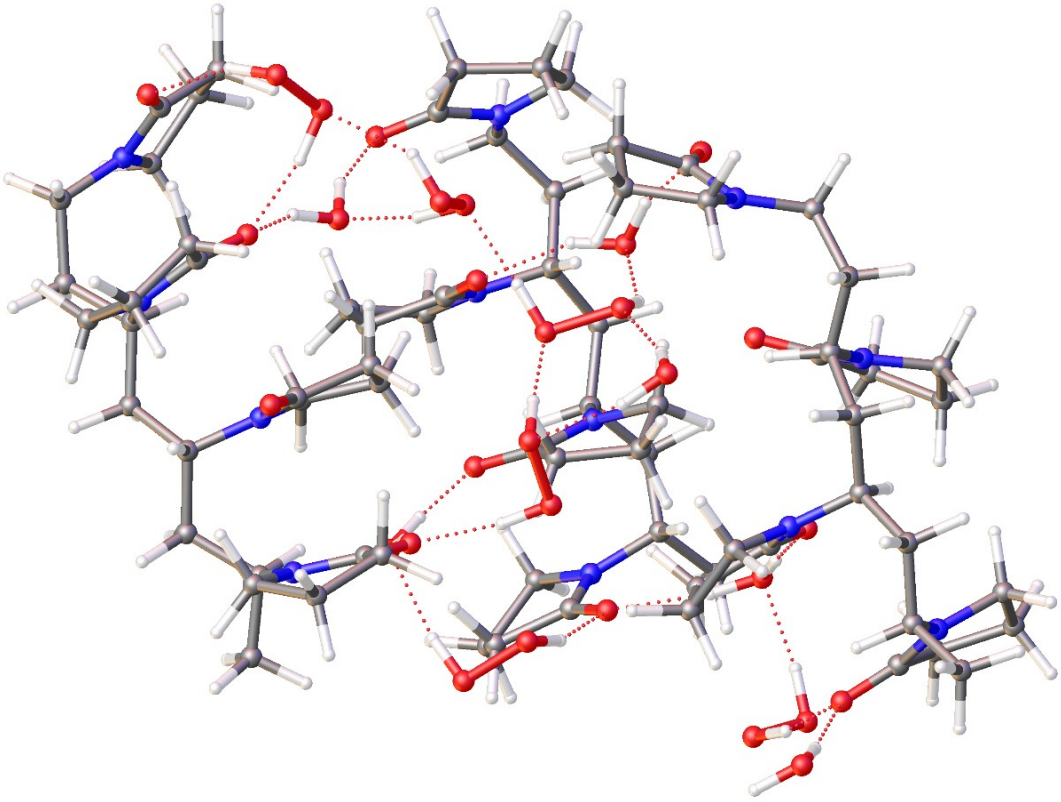

Figure S23. The DFT calculated structure of three PVP tetramer molecules with six water molecules at position B and six H_2O_2 molecules at A, forming two AB ribbons.

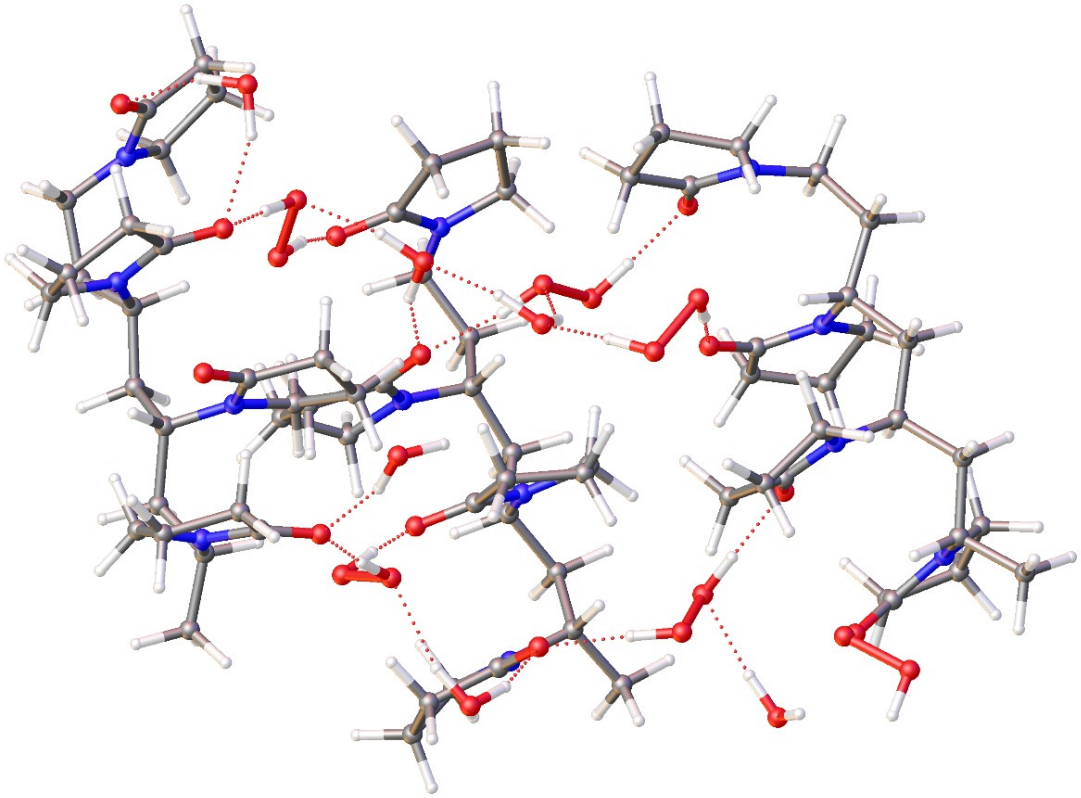

Figure S24. The DFT calculated structure of three PVP tetramer molecules with six water molecules at position A and six H_2O_2 molecules at B, forming two AB ribbons.

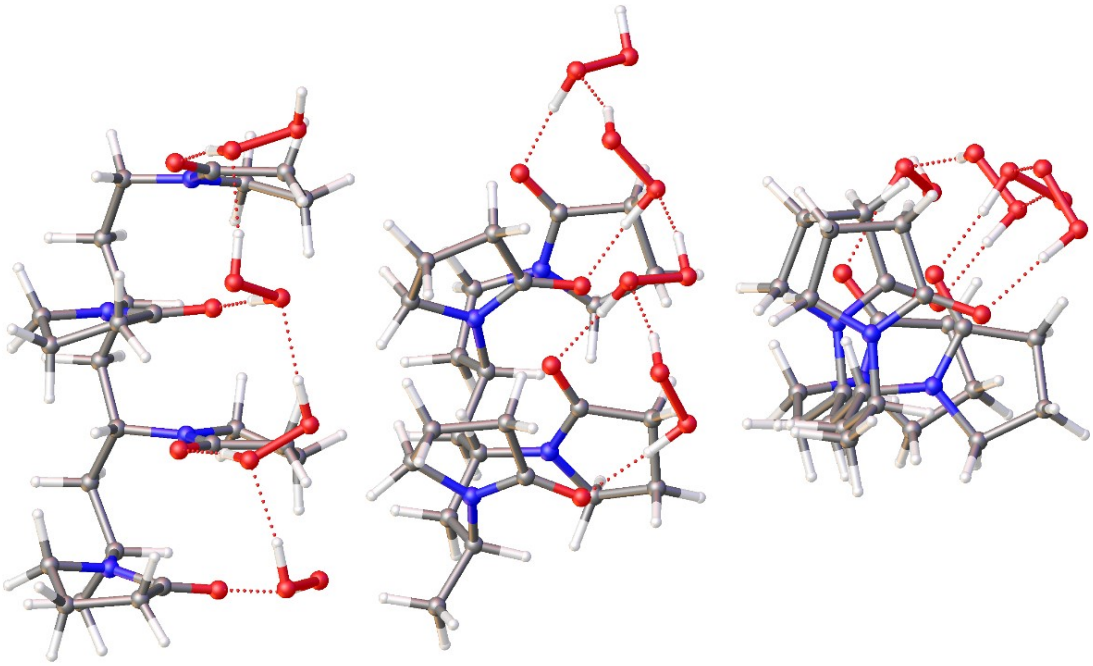

Figure S25. The DFT calculated structure of three PVP tetramer molecules with twelve H_2O_2 molecules, forming three all-A ribbons.

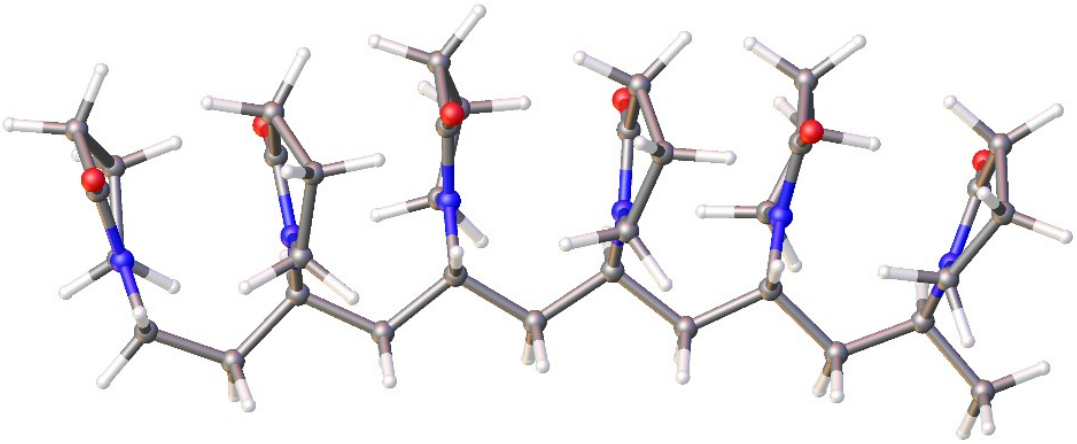

Figure S26. The DFT calculated structure of one PVP hexamer molecule.

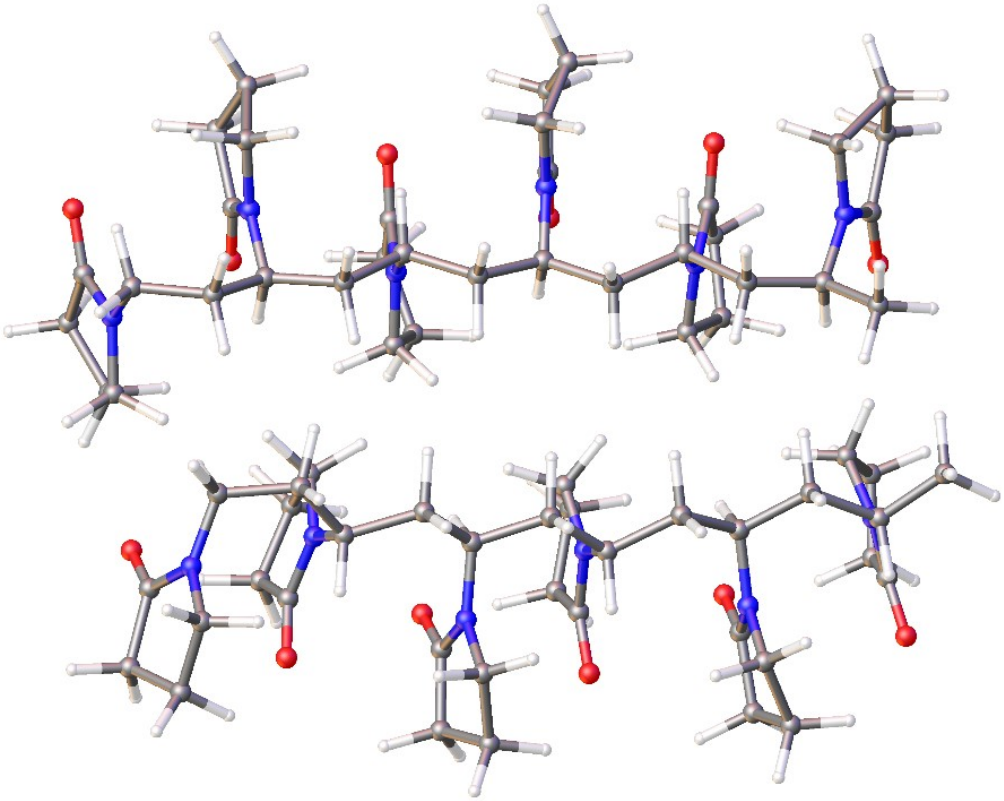

Figure S27. The DFT calculated structure of two PVP hexamer molecules.

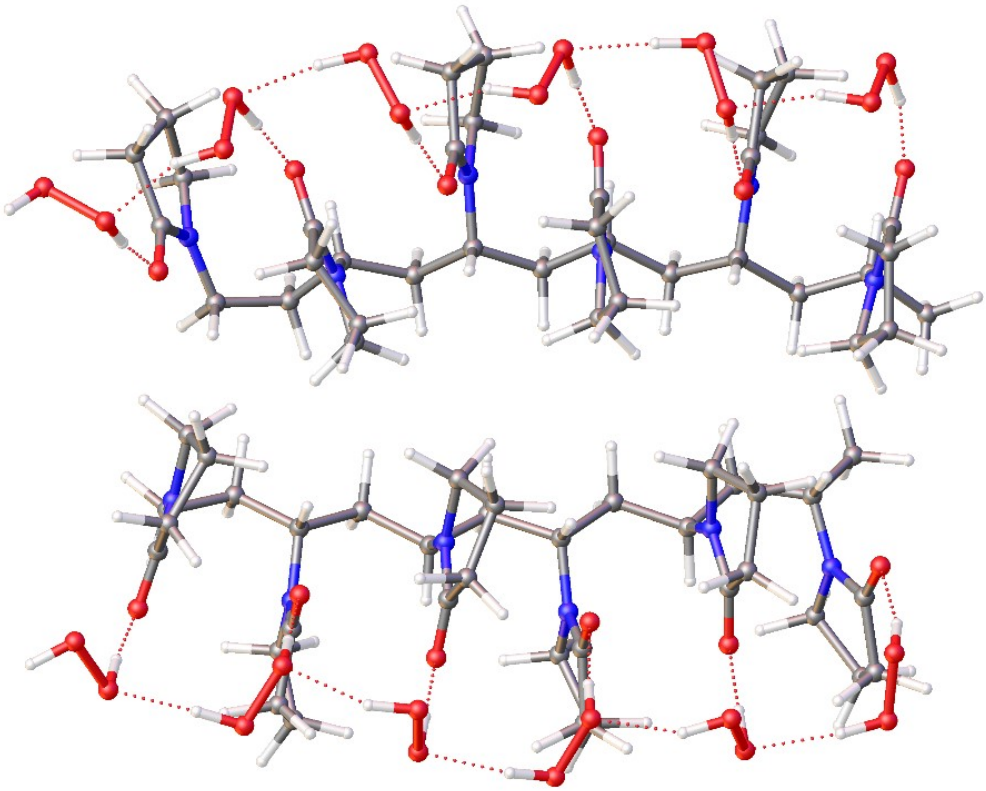

Figure S28. The DFT calculated structure of two PVP hexamer molecules with twelve H_2O_2 molecules, forming two all-A ribbons.

References

1. O. Maass and W. H. Hatcher, *J. Am. Chem. Soc.*, 1920, **42**, 2548-2569.
2. Y. Wolanov, O. Lev, A. V. Churakov, A. G. Medvedev, V. M. Novotortsev and P. V. Prikhodchenko, *Tetrahedron*, 2010, **66**, 5130-5133.
3. G. Sheldrick, *Acta Crystallogr. C*, 2015, **71**, 3-8.
4. O. V. Dolomanov, L. J. Bourhis, R. J. Gildea, J. A. K. Howard and H. Puschmann, *J. Appl. Crystallogr.*, 2009, **42**, 339-341.
5. L. J. Barbour, *Supramol. Chem.*, 2001, **1**, 189-191.
6. K. V. Titova, V. P. Nikol'skaya, V. V. Buyanov and I. P. Suprun, *Russ. J. Appl. Chem.*, 2002, **75**, 1903-1906.
7. M. J. Frisch, G. W. Trucks, H. B. Schlegel, G. E. Scuseria, M. A. Robb, J. R. Cheeseman, G. Scalmani, V. Barone, G. A. Petersson, H. Nakatsuji, X. Li, M. Caricato, A. V. Marenich, J. Bloino, B. G. Janesko, R. Gomperts, B. Mennucci, H. P. Hratchian, J. V. Ortiz, A. F. Izmaylov, J. L. Sonnenberg, Williams, F. Ding, F. Lipparini, F. Egidi, J. Goings, B. Peng, A. Petrone, T. Henderson, D. Ranasinghe, V. G. Zakrzewski, J. Gao, N. Rega, G. Zheng, W. Liang, M. Hada, M. Ehara, K. Toyota, R. Fukuda, J. Hasegawa, M. Ishida, T. Nakajima, Y. Honda, O. Kitao, H. Nakai, T. Vreven, K. Throssell, J. A. Montgomery Jr., J. E. Peralta, F. Ogliaro, M. J. Bearpark, J. J. Heyd, E. N. Brothers, K. N. Kudin, V. N. Staroverov, T. A. Keith, R. Kobayashi, J. Normand, K. Raghavachari, A. P. Rendell, J. C. Burant, S. S. Iyengar, J. Tomasi, M. Cossi, J. M. Millam, M. Klene, C. Adamo, R. Cammi, J. W. Ochterski, R. L. Martin, K. Morokuma, O. Farkas, J. B. Foresman and D. J. Fox, Gaussian 16, Revision B.01, Gaussian, Inc., Wallingford, CT, 2016
8. A. D. Becke, *J. Chem. Phys.*, 1993, **98**, 5648-5652.

9. C. Lee, W. Yang and R. G. Parr, *Phys. Rev. B*, 1988, **37**, 785-789.
10. G. A. Petersson, A. Bennett, T. G. Tensfeldt, M. A. Al-Laham, W. A. Shirley and J. Mantzaris, *J. Chem. Phys.*, 1988, **89**, 2193-2218.
11. G. A. Petersson and M. A. Al-Laham, *J. Chem. Phys.*, 1991, **94**, 6081-6090.
12. S. Grimme, S. Ehrlich and L. Goerigk, *J. Comp. Chem.*, 2011, **32**, 1456-1465.
13. J. P. Merrick, D. Moran and L. Radom, *J. Phys. Chem. A*, 2007, **111**, 11683-11700.
14. A. E. Aliev, D. Courtier-Murias and S. Zhou, *J. Mol. Struct.: THEOCHEM*, 2009, **893**, 1-5.